Electrochemical Study of Electron Transport through Thin DNA Films§

Gerhard Hartwich, Daren J. Caruana,† Thierry de Lumley-Woodyear,‡ Yubin Wu, Charles N. Campbell, and Adam Heller*

Contribution from the Department of Chemical Engineering and the Texas Materials Institute, The University of Texas at Austin, Austin, Texas 78712-1062

Received June 17, 1999

Abstract: The electron/hole conduction of disordered bulk double-stranded (ds) calf thymus DNA and of one-dimensionally aligned 12-base pair single- and double-stranded oligonucleotide monolayers on gold was probed by testing for the occurrence of Faradaic processes. The disordered ds-DNA film was probed by doping it with soybean peroxidase, an easy to "wire" thermostable polycationic enzyme and measuring the current density of electroreduction of H_2O_2 to water at SCE potential. Although the current density in films with hydrophilic electron-conducting polymeric "wires" is ~0.5 mAcm^{-2}, when ds-DNA was used to "wire" soybean peroxidase, the current density was only 0.1 μA cm^{-2}, similar to that in the absence of an electron-conducting enzyme-"wiring" polymer. We conclude that the diffusivity of electrons in unaligned and unstretched calf thymus DNA is less than 10^{-11} cm^2 s^{-1}. Nevertheless, the occurrence of a Faradaic reaction was observed in the Au−S−$(CH_2)_2$−ds-oligo-NH−PQQ/Au−S−CH_2−CH_2−OH monolayer on gold, in which the helices were one-dimensionally aligned and comprised a >30 Å ds-oligonucleotide segment. In these the rate constant for PQQ electrooxidation−electroreduction was 1.5 ± 0.2 s^{-1}, only about 4-fold less than the 5 ± 1 s^{-1} constant for the reference Au−S−$(CH_2)_2$−NH−PQQ monolayer. When two mismatches were introduced in the 12 base-pair ds-oligonucleotide (by C → A and C → T substitutions) the constant decreased to 0.6 ± 0.2 s^{-1}. In contrast, the rate for the Au−S−$(CH_2)_2$−ss-oligo-NH−PQQ/Au−S−CH_2−CH_2−OH monolayer was too small to be measured; no voltammetric waves were detected at a scan rate of 10 mV s^{-1}. The anisotropic conduction in the one-dimensionally ordered solid ds-DNA films is attributed to the concerted movement of cations in the direction of the main axes of the ds-helices when an electric field is applied. Such movement causes the high-frequency longitudinal (not the high-frequency transverse optical) polarizability to be high and thereby makes the resolved component of the high-frequency dielectric constant high. The solid ds-DNA films also contain less water than their solutions, which reduces the static dielectric constant relative to that of water. As shown by Mott and Gurney, reduction of the difference between the static dielectric constant and the high-frequency longitudinal dielectric constant increases the mean free path and the mobility of electrons in an ionic solid and makes ds-DNA a one-dimensional semiconductor. The high frequency dielectric constant, as described in textbooks on solid-state physics, also decreases the ionization energies of donors and greatly extends their Bohr-radii, which are sausage-shaped in ds-DNA. A likely n-type dopant is the G-base in the GC base pair, a dopant ionized ("oxidized") in the high-frequency dielectric constant medium. The proposed biological function of the insulator-to-semiconductor transition upon parallel alignment of the ds-DNA is protection against irreversible chemical change by oxidation or reduction. Removing or adding of an electron produces in an insulator a localized reactive radical. Adding a hole or an electron to a band of a semiconductor, which extends over a large number of atoms, does not make any atom in the ensemble uniquely reactive.

Introduction

The occurrence or absence of a Faradaic process (an electroreduction or an electrooxidation reaction) in an ion-conducting condensed phase is a rigorous test for transport, or absence of transport, of electron or holes: In the absence of an electron- or hole-transporting process a Faradaic reaction cannot take place, and the occurrence of a Faradaic process proves that electrons or holes are transported in the ion-conducting solid or liquid. Electrons or holes need not be transported as such for a Faradaic process to occur: They can be transiently bound to a member of a redox couple, referred to as a mediator, which may diffuse or be polymer-bound. Here we probe, through studying Faradaic processes, the transport of electrons or holes along the long axes of the double-stranded DNA and oligonucleotides helices, continuing experimental and theoretical

* To whom correspondence should be addressed.

† Current address: University College London, Department of Chemistry, 20 Gordon Street, London WC1 H0AJ, UK.

‡ Current address: Cambridge University, Center for Protein Engineering, Medical Research Council, Cambridge CB2 2QH, UK.

§ **Abbreviations.** PQQ, pyrrolo-quinoline-quinone (4,5-dihydro-4,5-dioxo-1H-pyrrolo-[2,3-*f*]-quinoline-2,7,9-tri-carboxylic acid); TEATFB, tetraethylammonium-tetrafuoroborate; sulfo-NHS, *N*-hydroxysulfosuccinimide; EDC, (3-dimethylaminopropyl)carbodiimide; HEPES, *N*-[2−hydroxyethyl] piperazine-*N*′-[2-ethanesulfonic acid]; hybridization solution: 10 mM Tris-hydroxymethylamine, 1 mM ethylenediamine tetraacetate, pH 7.5 containing 0.7 M TEATFB; Au−S−$(CH_2)_2$−NH_2, Au film on mica, with a covalently attached monolayer of cystamine; Au−S−$(CH_2)_2$-NH−PQQ, Au−S−$(CH_2)_2$−NH_2 with part of the terminal amines linked to the PQQ 7-carboxylic acid; Au−S−$(CH_2)_2$−ds-oligo-NH−PQQ/Au−S−CH_2−CH_2−OH, Au on mica onto which a monolayer of the double stranded PQQ modified oligonucleotide was anchored, the monolayer also containing Au−S−CH_2−CH_2−OH; Au−S−$(CH_2)_2$−ss-oligo-NH−PQQ, same, with the single -tranded PQQ modified oligonucleotide; SBP, soybean peroxidase; PEGDGE, poly(ethylene glycol) diglycidyl ether, MW 400. *ET*, electron transfer or transport; CV, cyclic voltammogram or voltammetry; E_0^a and E_0^c, anodic or cathodic peak potential; E_0, half wave potential; ν, scan rate; ΔE_p, the difference of the potentials of the maxima of the anodic and cathodic waves; E_{fwhh}, full width at half-height of a wave; SCE, saturated calomel electrode.

10.1021/ja9920664 CCC: $18.00
Published on Web 11/04/1999

work that spanned the past 37 years.[1−5] Fink and Schönenberger recently reported passage of electron or hole current through clusters of ds-DNA molecules ("ropes") in vacuo, finding that the characteristics of the transport resembled those of a semiconductor.[6] Okahata and colleagues found high and anisotropic conduction in densely packed, hydrated, and oriented films of DNA helices along their main axis, but not in the plane perpendicular to it.[7] Kelley and her colleagues reported long-range electron transfer across oriented ds-DNA monolayers in which daunomycin was intercalated and covalently bound to G-residues.[8] Earlier studies, mostly on DNA solutions in which DNA helices were aligned so that their long axes were parallel, exhibited electrical dichroism, birefringence, and anisotropic dielectric properties.[9−24] In solid films also spontaneous polarization and formation of ferroelectric domains were observed.[25] The chemical community became interested in the transfer of electrons across long distances in ds-oligonucleotides following the photoluminescence and photochemical studies of Barton, Turro, and their colleagues who found that the transfer remained rapid even when the separation of electron donors and acceptors was substantial.[26−30] Schuster and colleagues reported that this was the case also in peptide nucleic acid duplexes.[31,32] Meggers and colleagues discovered that the long-range transfer of electrons is conditional on properly spaced guanine residues.[33,34] Lewis et al.[35] and Fukui and Tanaka[36] reported, however, that the distance dependence of the electron-transfer rates did not always differ from that in proteins, and a theoretical model of Beratan and colleagues[37,38] also suggested that the distance dependence of the transfer rate is similar to that in proteins. Okada et al.[39] and Jortner et al.[40] raised the possibility of long-range carrier transport by a hopping mechanism.

Here we compare the rates of Faradaic reactions requiring transport of electrons or holes through disordered, bulk calf thymus ds-DNA and through aligned oligonucleotide monolayers on the [111] face of gold. The DNA was grafted onto the gold surfaces through a short (4.5 ± 0.5 Å) $-S-(CH_2)_2-$ spacer-arm, bound to the 3′-phosphate. The PQQ redox couple was covalently attached to primary amines of a $C-5'-CH_2-CH{=}CH-CO-NH-CH_2-CH_2-NH_2$ spacer, bound to a solution-side terminal thymine. A schematic drawing of the $Au-S-(CH_2)_2-$ds-oligo-NH−PQQ structure, the length of the main axis of which was 49 ± 2 Å, is shown in Figure 1.

Experimental Section

Gold Electrodes. Gold (99.99%) films of 100 nm thickness were sputtered on freshly cleaved and Ar plasma ion-etched muskovite mica faces, by the procedure of Rubinstein et al.[41,42] Immediately after the sputtering the films were annealed at 290 °C for 2.5 h and then allowed to cool over 1 h to room temperature. The geometrical area of the electrodes was 1 cm^2. To strip the impurities adsorbed during the annealing step, the gold films were cleaned in 30% H_2O_2/70% H_2SO_4, rinsed with DI-water, then soaked in absolute EtOH for 20 min (to reductively strip any chemisorbed O_2), and immediately immersed in and reacted with the monolayer-forming disulfide solution.

Monolayer Formation. The $Au-S-(CH_2)_2-NH_2$ monolayers were formed by immersing the Au films in 0.02 M cystamine for >2 h.[43] The $Au-S-(CH_2)_2-NH-$PQQ monolayers were formed by incubating the $Au-S-(CH_2)_2-NH_2$ electrodes in a solution of 3×10^{-3} M PQQ, 10 mM EDC, and 10 mM sulfo-NHS in pH 7.2 HEPES. This procedure leads to preferential condensation of the 7-carboxylic acid function of PQQ with amines of the monolayer.[44]

The $Au-S-(CH_2)_2-$ss-oligo-NH−PQQ/$Au-S-CH_2-CH_2-OH$ monolayer was formed as follows: 3′-ACGAAGGCTGAT-5′ oligonucleotide, mono-esterified with $(HO-CH_2-CH_2-S-)_2$ at the 3′-phosphate end and modified with a $-CH_2-CH{=}CH-CO-NH-CH_2-CH_2-NH_2$ function at the C-5 position of the 5′-thymine, was purchased from Genosys, The Woodlands, Texas. The disulfides of the hybrid were next reacted with the gold surface by immersing the gold electrode for >24 h in the solution containing all components of the hybridization solution except for the complementary oligonucleotide. Incubation with a solution of 3×10^{-3} M PQQ, 10 mM EDC, and 10 mM sulfo-NHS in pH 7.2 HEPES buffer led to preferential condensation of the 7-carboxylic acid function of PQQ[44] with the amine function at the 5′-thymine. Immobilization, other than by covalent attachment to the amine function at the 5′-thymine, did not take place. When the EDC coupling agent was omitted, the cyclic voltammograms did not show detectable PQQ peaks.

The double-stranded oligonucleotide monolayer, $Au-S-(CH_2)_2-$ds-oligo-NH−PQQ/$Au-S-CH_2-CH_2-OH$, was formed by a similar procedure, except that the 3′-ACGAAGGCTGAT-5′ oligonucleotide,

(1) Eley, D. D.; Spivey, D. I. *Trans. Faraday Soc.* **1962**, *58*, 411.
(2) Hofmann, T. A.; Ladik, J. *Adv. Chem. Phys.* **1964**, *7*, 84.
(3) Suhai, S. *J. Chem. Phys.* **1972**, *57*, 5599.
(4) Dee, D.; Baur, M. E. *J. Chem. Phys.* **1974**, *60*, 541.
(5) Mikac-Dadic, V.; Pravdic, V.; Rupprecht, A. *Bioelectrochem. Bioenerg.* **1974**, *1*, 364.
(6) Fink, H.-W.; Schönenberger, C. *Nature* **1999**, *398*, 407.
(7) Okahata, Y.; Kobayashi, T.; Tanaka, K.; Shimomura, M. *J. Am. Chem. Soc.* **1998**, *120*, 6165.
(8) Kelley, S. O.; Jackson, N. M.; Hill, M. G.; Barton, J. K. *Angew. Chem., Int. Ed.* **1999**, *38*, 941.
(9) Harrington, R. E. *J. Am. Chem. Soc.* **1970**, *92*, 6957.
(10) Hornick, C.; Weill, G. *Biopolymers* **1971**, *10*, 2345.
(11) Takashima, S. *Biopolymers* **1973**, *12*, 145.
(12) Hogan, M.; Dattagupta, N.; Crothers, D. M. *Proc. Natl. Acad. Sci. U.S.A.* **1978**, *75*, 195.
(13) Norden, B.; Davidsson, A. *Chem. Phys.* **1978**, *30*, 177.
(14) Marion, C.; Hanss, M. *Biopolymers* **1980**, *19*, 1629.
(15) Charney, E.; Yamaoka, K. *Biochemistry* **1982**, *21*, 834.
(16) Matsuda, K. *J. Sci. Hiroshima Univ., Ser. A: Phys. Chem.* **1983**, *47*, 41.
(17) Marion, C.; Roux, B.; Bernengo, J. C. *Makromol. Chem.* **1984**, *185*, 1647.
(18) Takashima, S.; Gabriel, C.; Sheppard, R. J.; Grant, E. H. *Biophys. J.* **1984**, *46*, 29.
(19) Altig, J. A.; Wesenberg, G. E.; Vaughan, W. E. *Biophys. Chem.* **1986**, *24*, 221.
(20) Yamaoka, K.; Fukudome, K. *J. Phys. Chem.* **1988**, *92*, 4994.
(21) Yamaoka, K.; Fukudome, K. *J. Phys. Chem.* **1990**, *94*, 6896.
(22) Rill, R. L.; Strzelecka, T. E.; Davidson, M. W.; Van Winkle, D. H. *Physica A* **1991**, *176*, 87.
(23) Voitylov, V. V.; Voskresenski, I. A. V.; Kakorin, S. A.; Trusov, S. A.; Trusov, A. A. *Biofizika* **1990**, *35*, 726.
(24) Washizu, H.; Kikuchi, K. *Chem. Lett.* **1997**, *7*, 651.
(25) Vasilescu, D. *Phys.-Chem. Prop. Nucleic Acids* **1973**, *1*, 31.
(26) Purugganan, M. D.; Kumar, C. V.; Turro, N. J.; Barton, J. K. *Science* **1988**, *241*, 1645.
(27) Murphy, C. J.; Arkin, M. R.; Jenkins, Y.; Ghatlia, N. D.; Bossmann, S. H.; Turro, N. J.; Barton J. K. *Science* **1993**, *262*, 1025.
(28) Holmlin, R. E.; Dandliker, P. J.; Barton, J. K. *Angew. Chem., Int. Ed. Engl.* **1997**, *36*, 2714.
(29) Hall, D. B.; Holmlin, R. E.; Barton, J. K. *Nature* **1996**, *382*, 731.
(30) Danliker, P. J.; Holmlin, R. E.; Barton, J. K. *Science* **1997**, *275*, 1465.
(31) Armitage, B. et al. *Proc. Natl. Acad. Sci. U.S.A.* **1997**, *94*, 12325.
(32) Casper, S. M.; Schuster, G. B. *J. Am. Chem. Soc.* **1997**, *119*, 12762.
(33) Meggers, E.; Kusch, D.; Spichty, M.; Wille, U.; Giese, B. *Angew. Chem., Int. Ed.* **1998**, *37*, 460.
(34) Meggers, E.; Michel-Beyerle, M. E.; Giese, B. *J. Am. Chem. Soc.* **1998**, *120*, 12950.
(35) Lewis, F. D.; Wu, T.; Zhang, Y.; Letsinger, R. L.; Greenfield, S. R.; Wasielewski, M. R. *Science* **1997**, *277*, 673.
(36) Fukui, K.; Tanaka, K. *Angew. Chem., Int. Ed.* **1998**, *37*, 158.
(37) Beratan, D. N.; Priyadarshy, S.; Risser, S. M. *Chem. Biol.* **1997**, *4*, 3.
(38) Priyadarshy, S.; Risser, S. M.; Beratan, D. N. *J. Phys. Chem.* **1996**, *100*, 17678.
(39) Okada, A.; Chernyak, V.; Mukamel, S. *J. Chem. Phys. A* **1998**, *102*, 1241.
(40) Jortner, J.; M.Bixon, M.; Langenbacher, T.; Michel-Beyerle, M. E. *Proc. Natl. Acad. Sci. U.S.A.* **1998**, *95*, 12759.
(41) Golan, Y.; Margulis, L.; Rubinstein, I. *Surf. Sci* **1992**, *264*, 312.
(42) Ron, H.; Matlis, S.; Rubinstein, I. *Langmuir* **1998**, *14*, 1116.
(43) Katz, E.; Schlereth, D. D.; Schmidt, H.-L. *J. Electroanal. Chem.* **1994**, *367*, 59.
(44) Willner, I.; Heleg-Shabtai, V.; Blonder, R.; Katz, E.; Tao, G.; Buckmann, A. F.; Heller, A. *J. Am. Chem. Soc.* **1996**, *118*, 10321.

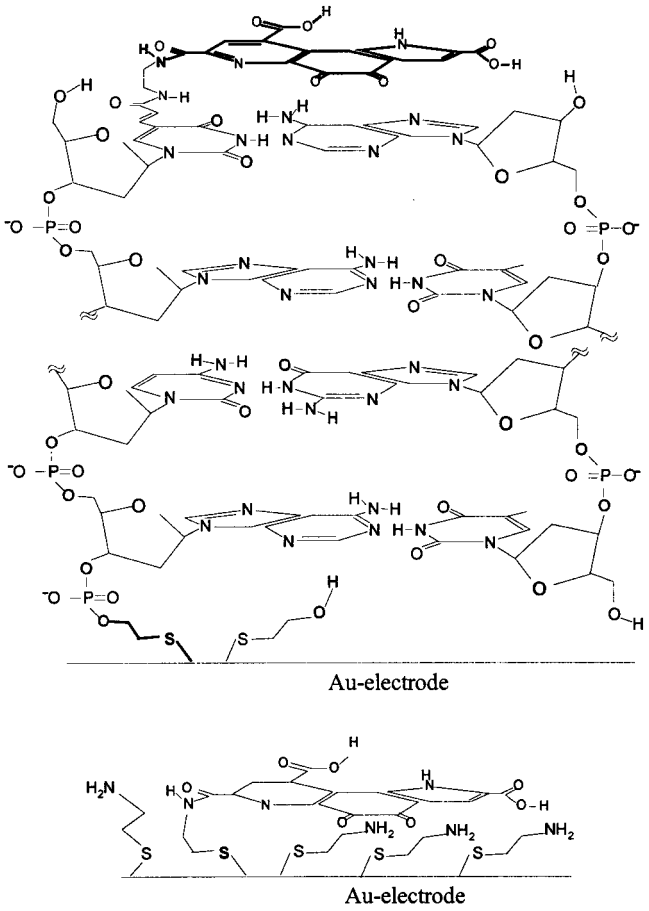

Figure 1. Top: Schematic drawing of the 12 base pair PQQ-bound ds-oligonucleotide (3′-ACGAAGGCTGAT-5′) hybrid on gold, Au−S−$(CH_2)_2$−ds-oligo-NH−PQQ. The PQQ redox function is attached to the 5′-thymine via a C-5-CH_2−CH═CH−CO−NH−CH_2−CH_2−NH_2 spacer arm. The length of the unit is ∼49 ± 2 Å. Geometry optimized using a 31-G* basis set[84] and by siting the PQQ π-plane in parallel with the base π-plane at a distance of 3.2 Å. The parallel alignment is in accord with experimental findings in similar systems.[85] Bottom: Schematic drawing of the structure of the related electrode Au−S−$(CH_2)_2$−NH−PQQ, which has no oligonucleotide. The remaining available gold surface is occupied by cystamine.

mono-esterified with (HO−CH_2−CH_2−S−)$_2$ at the 3′-phosphate end and modified with a −CH_2−CH═CH−CO−NH−CH_2−CH_2−NH_2 function at the C-5 position of the 5′-thymine 0.2 mM solution, was hybridized with an equal volume 0.2 mM of its nonesterified and unmodified complementary strand for 2 h at ambient temperature in the hybridization solution prior to reacting its disulfides with the gold surface. Incubation with a solution of 3×10^{-3} M PQQ, 10 mM EDC and 10 mM sulfo-NHS in pH 7.2 HEPES buffer led to preferential condensation of the 7-carboxylic acid function of PQQ[44] with the amine function of the spacer chain on the terminal 5′-thymine. Immobilization of PQQ, other than by covalent attachment to the terminal thymine, did not occur. When the EDC coupling agent was omitted, the cyclic voltammograms did not show detectable PQQ peaks.

Two mismatched base pairs were introduced in the Au−S−$(CH_2)_2$−ds-oligo-NH−PQQ hybrids by hybridizing with the 3′-TGCTTAT-GACTA-5′ imperfectly complementary oligonucleotide instead of the perfectly complementary 3′-TGCTTCCGACTA-5′-oligonucleotide. The procedure was identical with that through which the Au−S−$(CH_2)_2$−ds-oligo-NH−PQQ/Au−S−CH_2−CH_2−OH monolayer was formed except that the concentration of the oligonucleotide with two mismatched base pairs in the hybridization solution was 0.1mM.

Experiments on Bulk DNA. Calf thymus DNA (cat. no. D3664) and soybean peroxidase (cat. no. P1432) were obtained from Sigma, St. Louis, MO. Phosphate buffered test solution was made using Dulbecco's PBS (cat. no. 28374) from Pierce Chemical Co., Rockford, IL. Poly(ethylene glycol) diglycidyl ether (PEGDGE) cross-linker (cat. no. 08211) was purchased from Polysciences, Warrington, PA. All other reagents were purchased from Aldrich, Milwaukee, WI. The osmium-containing polymer was a copolymer of poly(acrylamide) and poly-(vinylimidazole) complexed with osmium 4,4′-dimethyl-2,2′-bipyridine.[45] The experiments were carried out in PBS containing 1 mM H_2O_2, using a 3 mm diameter vitreous carbon electrode. The electrode was rotated at 1000 rpm and poised at SCE potential.

The component coating solutions of the SBP electrodes were prepared as follows. The SBP solution (20 mg/mL in 0.1 M $NaHCO_3$) was mixed with an equal volume of a $NaIO_4$ (12 mg/mL in water) solution. The mixture was kept in the dark for 2 h, then centrifuged and washed with a copious volume of 0.1 M $NaHCO_3$ using a Microcon 30 concentrator. Calf thymus DNA (50 μl at 1.2 mg/mL in water) was mixed with 1 mL of methyl imidazole buffer (20 mM, pH7) containing 0.15 M EDC and 2.5 mM hydrazine monohydrate and reacted overnight (18 h) at room temperature. The treated DNA was then washed with methyl imidazole buffer in a Microcon concentrator. Electrodes were prepared by depositing 6 μl of 85 wt % DNA (2.93 mg/mL) or PAA−PVI−Os−Hz (5 mg/mL), 5 wt % PEGDGE (0.5 mg/mL) and 10 wt % SBP (9 mg/mL) onto the 3 mm glassy carbon electrodes. The electrodes were cured in a humid atmosphere for 16 h and then overnight in ambient air before testing. Prior to testing the electrodes were washed in PBS for 15 min.

Instrumentation. The CVs were measured with a computer-controlled low-noise bipotentiostat (CH Instruments, model 832) at ambient temperature in a standard three-electrode cell, with a coiled platinum wire auxiliary electrode and a double junction Luggin capillary Ag/AgCl (saturated KCl internal solution) or an SCE reference electrode. The electrolyte was pH 7.2 HEPES buffer with 0.7 M TEATFB. The modified electrodes were rinsed with DI water before the measurements. X-ray photoelectron spectra (XPS) were obtained with a Physical Electronics Phi model 5700 ESCA system, operated at 10^{-10} Torr, using monochromatic Al Kα X-rays at 1486.6 eV at 300 W with 2 mm focused filament. Its hemispherical analyzer was operated at a band-pass energy of 93.9 eV (survey scan, time/step = 0.2 s at 0.4 eV/step) or 11.75 eV (high-resolution scan, time/step = 1 s at 0.1 eV/step) with the entrance aperture (4 μm) at 45° relative to the sample surface.

Results

Experiments on Thin Films. Absence of Electrical "Wiring" of Horseradish Peroxidase by Randomly Oriented Double-Stranded DNA. Peroxidase-containing films of electron-conducting polymers catalyze the electroreduction of H_2O_2 to water.[46−51] SBP "wired" with the electron-conducting copolymer of poly(acrylamide) and [poly(vinylimidazole) complexed with osmium 4,4′-dimethyl-2,2′-bipyridine][45,48] produces a reduction current of 460 ± 57 μA/cm^2. Upon the attempted "wiring" of soybean peroxidase with calf thymus ds-DNA, the H_2O_2 electroreduction current was ∼5000 times lower, 0.1 μA/cm^2. The current density for cross-linked SBP without any "wiring" polymer was also 0.1 μA/cm^2.

Experiments on Monolayers. Surface Topology of the Gold Electrode Carrying the Oligonucleotide Monolayers. The micro-roughness of the gold surface was estimated by the method of Rand and Woods.[52] A gold oxide monolayer was formed by electrooxidizing the gold in 0.5 M H_2SO_4 (one

(45) de Lumley, T.; Rocca, P.; Lindsay, J.; Dror, Y.; Freeman, A.; Heller, A. *Anal. Chem.* **1995**, *67*, 1332.
(46) Vreeke, M. S.; Maidan, R.; Heller, A. *Anal. Chem.* **1992**, *64*, 3084.
(47) Vreeke, M. S.; Rocca, P.; Heller, A. *Anal. Chem.* **1995**, *67*, 303.
(48) Vreeke, M. S.; Yong, K. T.; Heller, A. *Anal. Chem.* **1995**, *67*, 4247.
(49) Bartlett, P. N.; Birkin, P. R.; Palmisano, F.; de Benedetto, G. *J. Chem. Soc. Faraday Trans.* **1996**, *92*, 3123.
(50) Bartlett, P. N.; Pletcher, D.; Zeng, J. *J. Electrochem. Soc.* **1997**, *144*, 3705.
(51) Bartlett, P. N.; Birkin, P. R.; Wang, J. H.; Palmisano, F.; de Benedetto, G. *Anal. Chem.* **1998**, *70*, 3685.
(52) Rand, D. A. J.; Woods, R. *J. Electroanal. Chem.* **1971**, *31*, 29.

oxygen atom is chemisorbed per surface gold atom corresponding to two electrons passed per gold atom at the electrooxidation/reduction). The charge passed in the electroreduction wave of the oxide to metallic gold was 550 ± 20 μC cm^{-2} (geometrical area). For the 2.9 Å nearest-neighbor distance on the gold [111] surface[53] the calculated charge density for electroreduction of the oxide monolayer, if the surface were perfectly smooth, would have been 440 μC cm^{-2}. The estimated roughness factor for the gold surfaces was therefore (550 ± 20)/440 = 1.25 ± 0.05.

Surface Density of Thiols. The surface density of Au−SR bonds in the Au−S−$(CH_2)_2$−NH_2 monolayer was estimated coulometrically as described by Widrig, Chung, and Porter.[54] By subtracting from the integrated anodic wave of the first CV (where the 2-aminoethanethiolate in Au−SR is oxidatively desorbed from the surface and gold oxide is formed), the cathodic wave of the first return (where the formed gold oxide is reduced). The difference between anodic and cathodic first wave charges was (400 ± 100) μC cm^{-2} corresponding to a coverage by 6.5 ± 1.5 × 10^{14} thiols cm^{-2} (actual area) and a nearest-neighbor distance of 4.5 ± 0.5 Å. These values were identical with those observed for monolayers of short chain alkanethiolates on gold of similar roughness[54,55] and close to the theoretically expected value of 4.9 Å expected for a densely packed, crystalline monolayer of long chain alkanethiolates tilted at 30 °C on gold [111].[54] For the second and following CV cycles the charges of the anodic and cathodic waves were identical, showing quantitative oxidative stripping of the thiol monolayer in the first oxidation wave.

Surface Density of the PQQ-Functions. With the microroughness and the density of thiols known, the coverage by bound PQQ was estimated from the charge passed in the electroreduction/oxidation of surface-bound PQQ/PQQ^{2-}. For the Au−S−$(CH_2)_2$−NH−PQQ monolayer integration yielded 7.3 μC cm^{-2} for the actual electrode area, corresponding to coverage by 2.3 × 10^{13} molecules cm^{-2}. For Au−S−$(CH_2)_2$−ds-oligo-NH−PQQ the integral was 1.5 μC cm^{-2} for the actual area corresponding to coverage by 4.7 × 10^{12} molecules cm^{-2}.[56]

Additional information about the topology of the Au−S−$(CH_2)_2$−ds-oligo-NH−PQQ/Au−S−CH_2−CH_2−OH monolayer was obtained from XPS measurements (Figure 2). XPS measurements report on the X-ray intensity absorbed by a certain element and thus, on the concentration of this element in the sample. The P:N:O:C ratio in the Au−S−$(CH_2)_2$−ds-oligo-NH−PQQ/Au−S−CH_2−CH_2−OH scan was 0.2:1:2:5, close to the theoretical ratio 0.2:1:2:3 ratio expected for the oligonucleotide monolayer, except for the disproportionately high carbon content, attributed to the presence of tetraethylammonium ions, originating in the 0.7 M TEATFB hybridization solution, in the film. The surface density of nitrogen atoms was 6.1 × 10^{14} nitrogen atoms cm^{-2}, and the measured ratio of the Au-4f/N-1s peaks was ∼2.

Electron Transport Characteristics. To avoid intercalation or electrostatic binding the polyanionic diffusional Fe(CN)$_6^{3-/4-}$ [58]

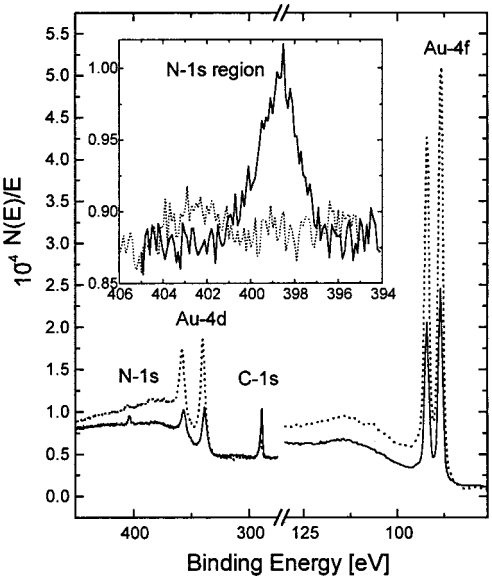

Figure 2. X-PS survey scans for Au−S−$(CH_2)_2$−NH−PQQ (- - -) and Au−S−$(CH_2)_2$−ds-oligo-NH−PQQ/Au−S−CH_2−CH_2−OH (—). Inset: Expansion of the N-1s region (The difference in peak positions is caused by different charging of the samples).

and covalently bound also polyanionic (PQQ) redox couples were chosen as probes. Kelley et al. found that the electroreduction/oxidation of Fe(CN)$_6^{3-/4-}$ did not produce measurable voltammetric waves at 100 mV s^{-1} scan rate on (111) gold faces after chemisorption of 6-carbon spacer arm 5′SH−$(CH_2)_6$−p−(15-base) oligonucleotides.[58] The cyclic voltammograms of Fe(CN)$_6^{3-/4-}$ on the 2-aminoethanethiolate (Au−S−$(CH_2)_2$−NH_2) electrode show that the monolayer did not block the transport of electrons, the separation of the electroreduction and electrooxidation peaks, ΔE_p, being 60 mV, close to the 59 mV theoretical value for a Nernstian, diffusion-limited, electrochemically reversible, one-electron redox system.[59] The Au−S−$(CH_2)_2$−ss-oligo-NH_2/Au−S−CH_2−CH_2−OH monolayer totally blocked (ΔE_p > 500 mV) electron exchange with Fe(CN)$_6^{3-/4-}$. In contrast, the Au−S−$(CH_2)_2$−ds-oligo-NH_2/Au−S−CH_2−CH_2−OH monolayer, generated by hybridizing the very same Au−S−$(CH_2)_2$−ss-oligo-NH_2 monolayer/Au−S−CH_2−CH_2−OH, blocked much less the exchange of electrons with Fe(CN)$_6^{3-/4-}$ (ΔE_p > 220 mV) showing that carrier transport through the film, or through pinholes in it, was now rapid.[60]

Ruling Out Pinhole Effects. Finklea, Rubinstein and their co-workers studied the characteristics of pinholes in octadecanethiol monolayers on gold. They showed that the voltammetric characteristics of pinholes differ from those of conventional macroelectrodes, resembling those of microarray electrodes.[61] The observed voltammograms with Fe(CN)$_6^{3-/4-}$ had the characteristics of conventional macroelectrodes, not of microarray electrodes.

To further rule out the possibility that the reduced attenuation of carrier transport in the double-stranded oligonucleotide monolayer was caused by pinholes, through which Fe(CN)$_6^{3-/4-}$ might have diffused, the transfer of charge was probed in monolayers with anionic PQQ redox functions covalently bound to the solution side termini of their oligonucleotides. The PQQ functions were attached to primary amines of spacer chains

(53) Hallmark, V. M.; Chiang, S.; Rabolt, J. F.; Swalen, J. D.; Wilson, R. J. *Phys. Rev. Lett.* **1987**, *59*, 2879.

(54) Widrig, C. A.; Chung, C.; Porter, M. D. *J. Electroanal. Chem.* **1991**, *310*, 335.

(55) Widrig, C. A.; Alves, C. A.; Porter, M. D. *J. Am. Chem. Soc.* **1991**, *113*, 2805.

(56) Subsequent scans were identical to the first scan for the Au−S−$(CH_2)_2$−NH2 electrode. For the Au−S−$(CH_2)_2$−ss-oligo-NH_2 electrode and the Au−S−$(CH_2)_2$−ds-oligo-NH_2 the peak current gradually increased, and ΔE_p decreased in the subsequent scans. This effect shows damage to the film upon repeated cycling.

(57) Finegold, L.; Donnell, J. T. *Nature* **1979**, *278*, 443.

(58) Kelley, S. O.; Barton J. K.; Jackson, N. M.; Hill, M. G. *Bioconjugate Chem.* **1997**, *8*, 31.

(59) Bard, A. J.; Faulkner, L. R. *Electrochemical Methods: Fundamentals and Application*; Wiley: New York, 1980.

(60) Laviron, E. *J. Electroanal. Chem.* **1979**, *101*, 19.

(61) Finklea, H. O.; Snider, D. A.; Fedyk, J.; Sabatani, E.; Gafni, Y.; Rubinstein, I. *Langmuir* **1993**, *9*, 3660.

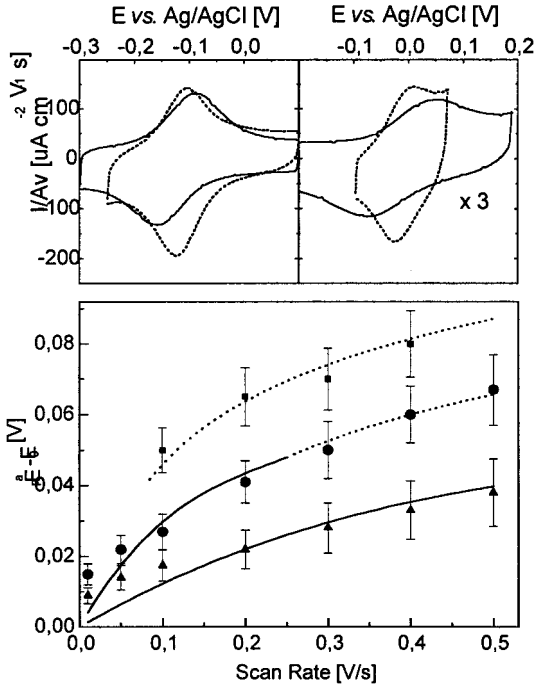

Figure 3. Top: Cyclic voltammograms, normalized for the scan rate, for the electrooxidation/reduction of PQQ/PQQ^{2-} functions bound to the termini of monolayers on gold. Au−S−$(CH_2)_2$−NH−PQQ (left) and Au−S−$(CH_2)_2$−ds-oligo-NH−PQQ/Au−S−CH_2−CH_2−OH (right) at $\nu = 10$ mV s^{-1} (···) and 500 mV s^{-1} (—). Bottom: Dependence of $E_p^a - E_0$ on the scan rate ν: experimental data for Au−S−$(CH_2)_2$−NH−PQQ (▲), Au−S−$(CH_2)_2$−ds-oligo-NH−PQQ/Au−S−CH_2−CH_2−OH (●), Au−S−$(CH_2)_2$−ds-oligo-NH−PQQ with a two base pair mismatch (■) and their fit to eq 3 (—) or to eq 4 (···). The error bars represent the RSD for a series of similarly made electrodes.

bound to the 5′-thymine bases at the solutions side-termini of the oligonucleotides. While such attachment prevented the diffusion of the redox couple through possible pinholes, it would have allowed their electrooxidation and electroreduction if the oligonucleotides, whether single- or double-stranded, were lying flatly or nearly flatly on the surface. It would, however, not have allowed electrooxidation/reduction of the PQQ couple if the double-stranded helices were perpendicular to, or were tilted only at a small angle relative to, normal. (Figure 1)

Faradaic Reaction in ds-Oligonucleotide Monolayers, Absence of Faradaic Reaction in ss-Oligonucleotide Monolayers and Retardation of the Rate of the Faradaic Reaction rate in ds-Monolayers with Mismatched Base Pairs. The observed electrooxidation/electroreduction of the single-stranded electrode Au−S−$(CH_2)_2$−ss-oligo-NH−PQQ was so slow that at a scan rate of $\nu = 10$ mV s^{-1} no voltammetric waves were seen. The CVs for the Au−S−$(CH_2)_2$−NH−PQQ and Au−S−$(CH_2)_2$−ds-oligo-NH−PQQ monolayers are shown in Figure 3 (top). The CV of the Au−S−$(CH_2)_2$−NH−PQQ monolayer was similar to that reported,[43] except for a difference in its nominal redox potential, which was 0.05 V vs Ag/AgCl at pH = 7, versus the reported − 0.12 V.[44] The dependence of the separation of the electrooxidation and electroreduction peaks, ΔE_p on the scan rate υ is shown, for Au−S−$(CH_2)_2$−ds-oligo-NH−PQQ, at the bottom of Figure 3.

To reconfirm that hybridization did indeed enhance the rates of electroreduction and electrooxidation of PQQ-functions covalently bound to the solution-side termini of the Au−S−$(CH_2)_2$−ss-oligo-NH−PQQ/Au−S−CH_2−CH_2−OH monolayers, imperfect hybrids with two mismatched based pairs were formed. The two mismatches were introduced by replacing the fully complementary oligonucleotide, TGCTTCCGACTA, with the TGCTTATGACTA sequence. The dependence of ΔE_p on the scan rate υ for the defective hybrid is shown at the bottom of Figure 3. As seen in the Figure, the separation of the anodic and cathodic peaks was significantly increased upon mismatching two base pairs in the 12-base hybrid.

Discussion

Absence of Electron or Hole Conduction in Disordered ds-Calf Thymus DNA: Confirming That in Absence of Chain-Alignment Bulk Double-Stranded DNA Is Not an Electrical Conductor, the Diffusivity of Electrons and Holes Being Less than 10^{-11} cm^2 sec^{-1}. Because of transport of cations, particularly of protons, characterization of the diffusion of electrons or holes through a hydrated DNA matrix requires special tools. One of these is the measurement of rates of Faradaic (electrooxidation or electroreduction) reactions. While Faradaic reactions do require transport of ions, they do not take place unless electrons or holes are also transported. The particular Faradaic process that was chosen for assessing the transport of holes or electrons through ds-DNA was the electroreduction of H_2O_2 to water

$$H_2O_2 + 2H^+ + 2e^- \rightarrow 2H_2O \qquad (1)$$

This reaction takes place in films comprising a peroxidase and a hydrated and electron conducting polymer (such as polyaniline, or a copolymer of $[Os(bpy)_2\ Cl]^{+/2+}$ complexed poly(*N*-vinyl imidazole)).[46−51] Peroxidases, with near-surface heme functions, are also electrooxidized/reduced on carbon electrodes in absence of a hydrated electron-conducting polymer, but only when oriented so as to bring the heme-function to the proximity of the electrode surface. In contrast, in a hydrated electron-conducting polymer film all heme centers are electroactive, irrespective of their orientation. The electrocatalytic H_2O_2 reduction currents are about 1000-fold higher in hydrated electron-conducting polymers with electron or hole diffusivities of $\sim 10^{-8}$ cm^2 s^{-1} than they are in the absence of an electron-conducting hydrophilic polymer. As seen in the Results, when soybean peroxidase, a polycationic enzyme (isoelectric point 9.5) was embedded in the polyanionic ds-calf thymus DNA matrix, the current density of H_2O_2 electroreduction did not exceed that seen in absence of an electron-conducting polymer, remaining in both cases 0.1 μA cm^{-2}. Because immobilization of soybean or horseradish peroxidase in an electron-conducting polymer resulted in a current density of $\sim 460 \pm 57$ μA cm^{-2}, the diffusivity of electrons or holes in the matrix comprising randomly oriented calf thymus DNA helices was less than 10^{-11} cm^2 s^{-1}. We conclude that addition of randomly oriented, hydrated, double-stranded DNA did not contribute to the transport of either electrons or holes.

Faradaic Processes Involving Electrons or Holes Passing Through a ~50 Å Thick Double-Stranded Oligonucleotide Monolayer: Why the PQQ Functions Could Not Be On or Near the Gold Surface; and Why, Even if the Monolayers Would Have Had some Pinholes, the Faradaic Processes Observed Could Not Have Resulted from These. In this section, we analyze the structure of the aligned, PQQ-terminated double-stranded monolayers, which we find to be densely packed, point out that the peaks/areas of the voltammetric waves were much larger than expected for pinholes, and point out that the observed increase in the separation of the anodic and cathodic peaks upon mismatching two base pairs could not be explained by a Faradaic process at pinholes.

Structures of related thiol-terminated ds-oligonucleotide monolayers on gold were analyzed by neutron scattering[64] and other methods.[69] The earlier studies, like this one, show that the helices are parallel, densely packed, and tilted at an angle of 30 ± 10° versus the normal to the gold surface on which they are randomly distributed. The densely packed Au−S−$(CH_2)_2$−NH_2 monolayer is crystalline.[41,42] Establishment of an ordered structure is attributed to the ability of the S−$(CH_2)_2$−NH_2 groups to migrate and thereby re-organize on the gold surface as the coverage increases while the monolayer forms. In contrast, the PQQ overlayer of the Au−S−$(CH_2)_2$−NH_2 baselayer, formed by reacting the activated carboxylate of PQQ with part of the monolayer's amines, cannot re-organize while the surface density of covalently bound PQQ increases and must be disordered. At maximal packing, randomly distributed nonoverlapping disks can cover one-half of a surface.[57] The surface, when packed with randomly distributed 16 Å disks of hydrated PQQ in the layer-forming process, can contain up to 2.5×10^{13} PQQ molecules cm^{-2}, a value close to the coulometrically measured coverage of 2.3×10^{13} molecules cm^{-2}.

AFM investigations of DNA[62] have shown that the diameter of hydrated double-stranded β-helices is about 35 Å. This would also be the diameter of their circular footprints if their long axes were perpendicular to the gold surface. The calculated maximal surface density for randomly distributed nonoverlapping 35 Å diameter disks is 5.2×10^{12} molecules cm^{-2}. It is identical with the surface density of $5.2 \pm 0.8 \times 10^{12}$ molecules cm^{-2} reported by Peterlinz et al.,[63] who measured the density by surface plasmon resonance, and by Steel et al.,[64] who measured it by redox marker intercalation in mixed monolayers with 6-mercaptohexanol. Levicky et al. analyzed the structures of the monolayers by neutron scattering.[65] They found that the monolayers are compact and that the DNA molecules "stand" on the gold surface or are at a small angle relative to the normal to it. In this study the coulometrically measured coverage in the mixed ds-oligonucleotide monolayers with 2-mercaptoethanol was 4.7×10^{12} molecules cm^{-2}, within the experimental error of the coverage reported by Peterlinz et al.[63] The value is consistent with tilting of the parallel helices at an angle of 30 ± 10° versus the normal to the gold surface.[66] The observed surface density provides firm evidence against the helices "lying" flatly on the gold surface. If they were, their footprint would have been 35 × 60 Å (60 Å being the sum of the 49 ± 2 Å length of the ds-oligonucleotide, the two spacer arms and of the PQQ molecule). At maximal packing, disordered nonoverlapping 35 × 60 Å cylinders can cover up to 0.56 of a surface.[57] Such coverage would have allowed the presence of up to 2.7×10^{12} Au−S−$(CH_2)_2$−ds-oligo-NH−PQQ molecules cm^{-2}. The coulometrically measured surface density of 4.7×10^{12} molecules cm^{-2} rules out such a structure.

The observed ratio of the peaks in the photoelectron spectra was consistent with the ratio expected for a "standing" Au−S−$(CH_2)_2$−ds-oligo-NH−PQQ/Au−S−CH_2−CH_2−OH monolayer, except for the higher than theoretical carbon-content, attributed to incorporation of tetraethylammonium cations from the 0.7 M TEATFB hybridization solution. The thickness of this monolayer can be estimated from its measured nitrogen content and from the measured Au -4f/N-1s ratio. For the Au−S−$(CH_2)_2$−ds-oligo-NH−PQQ/Au−S−CH_2−CH_2−OH monolayer, the calculated nitrogen content is 6.1×10^{14} nitrogen atoms cm^{-2}. This value is that calculated for a packed array of "standing" helices normal to the gold surface with 5.2×10^{12} helices per cm^2 and with 118 nitrogen atoms per helix. The value would have been 3.2×10^{14} nitrogen atoms cm^{-2} for "flatly lying" helices (at 2.7×10^{12} helices cm^{-2} and 118 nitrogen atoms/helix). For the nearest neighbor distance of 2.9 Å on gold [111][53] and for the distance of 2.5 Å between neighboring [111] planes, the experimental ratio of the Au -4f/N-1s peaks of ~2 corresponds to a penetration of about one layer of gold atoms in the case of the perpendicular helices and of less than half a gold layer atom in the case of the flatly lying helices, the penetration depth of the excitation beam in the latter case being about 25−30 Å (the estimated maximum diameter of the counterion-packed nonhydrated DNA), well below the actual penetration depth of the XPS-setting of at least 38 Å.[67] The measured surface density of 4.7×10^{12} molecules cm^{-2} and the photoelectron spectra are thus consistent with an array of helices tilted at angle of less than 40° relative to normal.

If the helices were tilted at an angle less than 40° and there were some pinholes, then only a small fraction of the PQQ functions could have been in contact with the surface, and the integral of the PQQ voltammetric waves would have been much smaller than that observed, which was close to that expected for an oligonucleotide monolayer.[63] Also, if the cause of the observed Faradaic reactions were pinholes, the voltammetric peaks would not have been nearly as much separated as was observed, the separation approaching nil in the case of a surface-bound fast and reversible redox couple. Furthermore, there would have been no plausible explanation of the increase in the separation of the anodic and the cathodic peaks in the voltammograms upon introduction of two mismatched base pairs in a sequence of 12 base pairs.

Rate Constants of the Electrochemical Reactions of $Fe(CN)_6^{3-/4-}$ and Rates of the Electrochemical Reactions of PQQ Functions Covalently Bound to the Solution Side Termini of the Chains: Transport of Electrons or Holes through the Monolayers Increases upon Hybridization and Is Reduced When the Hybrid Is Imperfect. Equations 2−4 relate[60,68] the kinetics of electrode reactions with ΔE_p, the measured potential difference between the peak of the electrooxidation current and the peak of the electroreduction current in a cyclic voltammogram. The rate constants k_0 for the electrode reaction of the diffusional redox couple, $Fe(CN)_6^{3-/4-}$, were calculated from eq 2,[68] in which D is the diffusivity of the redox couple in $cm^2\ s^{-1}$, ν is the scan rate in V s^{-1}, n is the number

(62) Zhu, J. Y. http://www.molec.com/apps **(**accessed 1999).

(63) Peterlinz, K. A.; Georgiadis, R. M.; Herne, T. M.; Tarlov, M. J. *J. Am. Chem. Soc.* **1997**, *119*, 3401.

(64) Steel, A. B.; Herne, T. M.; Tarlov, M. J. *Anal. Chem.* **1998**, *70*, 4670.

(65) Levicky, R.; Herne, T. M.; Tarlov, M. J.; Satija, S. K. *J. Am. Chem. Soc.* **1998**, *120*, 9787.

(66) With an ellipsoidal footprint of π(17.5 Å)^2/cos(θ) per tilted oligonucleotide the estimated angle of tilt for the measured coverage of 4.7×10^{12} molecules cm^{-2} is about 25° when a maximum packing fraction of 0.5 is assumed. Although there was no justification to choose a packing fraction of 0.5, the packing value could not have been greater than 0.56, nor smaller than 0.5. Assuming a packing value of 0.56 and using the lower limit of 1.2 μC cm^{-2} for the charge passed in the electroreduction/oxidation of PQQ/PQQ^{2-} in Au−S−$(CH_2)_2$−ds-oligo-NH−PQQ (worst case situation) the calculated angle of tilt would not have exceeded 50°.

(67) A minimal penetration depth of 38 Å was estimated from comparison with the denser reference system Au−S−$(CH_2)_2$−NH−PQQ, the photoelectron spectrum of which was measured simultaneously on the same sample holder under identical conditions. For Au−S−$(CH_2)_2$−NH−PQQ the nitrogen content of the monolayer was 7×10^{14} nitrogen atoms cm^{-2} (6.5×10^{14} nitrogen atoms cm^{-2} for the aminoethanethiolate monolayer and an overlayer with 2.3×10^{13} PQQ-functions cm^{-2}, containing 2 nitrogens each). The Au-4f/N-1s ratio in Au−S−$(CH_2)_2$−NH−PQQ of ~21 results in the penetration of the ~10 Å thick PQQ−aminoethanethiolate layer and 11 layers of gold (28 Å).

(68) Nicholson, R. S. *Anal. Chem.* **1965**, *37*, 1351.

(69) Herne, T. M.; Tarlov, M. J. *J. Am. Chem. Soc.* **1997**, *119*, 8916.

of electrons transferred, and F, R, and T have their usual meanings. Values of Ψ (eq 2) for different scan rates are provided by Nicholson.[68]

For a covalently surface immobilized redox couple Laviron[60] has shown that the heterogeneous rate constant, k_0, for electron transfer between the couple and the electrode can also be obtained from ΔE_p and υ. The values of k_0, ΔE_p, and υ are related through eq 3 when $\Delta E_p < 200$ mV and through eq 4 when $\Delta E_p > 200$ mV. Values of m (eq 3) for different scan rates are provided by Laviron.[60]

$$k_0 = \Psi \bullet \left(D \bullet \pi \bullet \nu \bullet \frac{nF}{RT}\right)^{1/2} \quad (2)$$

$$k_0 = \frac{mnF\nu}{RT} \quad (3)$$

$$\log k_0 = \alpha \log(1-\alpha) + (1-\alpha)\log \alpha - \log\left(\frac{RT}{mF\nu}\right) - \alpha(1-\alpha)\frac{nF\Delta E_p}{2.3RT} \quad (4)$$

When $Fe(CN)_6^{3-/4-}$ ($D \approx 10^{-5}$ cm^2 s^{-1}) was electroreduced/electrooxidized at $\nu = 10$ mV s^{-1}, ΔE_p was 60 mV for the Au−S−$(CH_2)_2$−NH_2 electrode. For the electrode with the Au−S−$(CH_2)_2$−ss-oligo-NH_2 monolayer no voltammetric waves were detected at $\nu = 10$ mV s^{-1}; in the case of the Au−S−$(CH_2)_2$−ds-oligo-NH_2 monolayer ΔE_p was 220 mV at $\nu = 10$ mV s^{-1}. The resulting values of k_0 were 4×10^{-2} cm s^{-1} for the Au−S−$(CH_2)_2$−NH_2 monolayer, ~0 cm s^{-1} for the Au−S−$(CH_2)_2$−ss-oligo-NH_2 monolayer and 2×10^{-3} cm s^{-1} for the Au−S−$(CH_2)_2$−ds-oligo-NH_2 monolayer.

The results for electrodes with PQQ covalently bound to the solution side of their monolayers were consistent with those obtained with the diffusing $Fe(CN)_6^{3-/4-}$ couple. The electrooxidation/electroreduction waves of the Au−S−$(CH_2)_2$−ds-oligo-NH−PQQ/Au−S−CH_2−CH_2−OH electrodes resembled those of the Au−S−$(CH_2)_2$−NH−PQQ electrode at $\upsilon = 10$ mV s^{-1} (Figure 3, top). In contrast, no voltammetric waves were detected at $\upsilon = 10$ mV s^{-1} when the electrode was modified with the single-stranded Au−S−$(CH_2)_2$−ss-oligo-NH−PQQ/Au−S−CH_2−CH_2−OH monolayer. Under the conditions of the experiment the single stranded oligonucleotide was stretched by internal electrostatic repulsion.[69] The 12 base pair ss-oligonucleotide effectively prevented electron and hole transport between the gold surface and the PQQ bound to the solution side of the films. For the Au−S−$(CH_2)_2$−NH−PQQ and the Au−S−$(CH_2)_2$−ds-oligo-NH−PQQ/Au−S−CH_2−CH_2−OH electrodes (Figure 3, top) the oxidation and reduction peak currents were equal, showing that the electrochemical transfer coefficient, α, was ~0.5 (eq 4). The peak currents scaled linearly with the scan rate through the 10−500 mV s^{-1} range, a behavior characteristic of surface immobilized redox couples. The dependence of the values of the differences between the potentials of the peaks of the PQQ^{2-} electrooxidation waves (E^a_p) and the redox potential of the PQQ^{2-}/PQQ couple, E_0 (which equal one-half of the ΔE_p values) on the scan rate is shown at the bottom of Figure 3. The figure also shows the correlation between the experimentally observed scan rate dependences of the potential differences $E^a_p - E_0$ and those calculated according to Laviron. The best fitting value of k_0 was 5 ± 1 s^{-1} for the electrode with the Au−S−$(CH_2)_2$−NH−PQQ monolayer, a value similar to the one reported;[43] for Au−S−$(CH_2)_2$-ss-oligo-NH−PQQ monolayer k_0 was ~0 s^{-1}; for the Au−S−$(CH_2)_2$-ds-oligo-NH−PQQ monolayer it was 1.5 ± 0.2 s^{-1}; and for Au−S−$(CH_2)_2$-ds-oligo-NH−PQQ monolayer with two mismatched base pairs (by CC_AT substitution), k_0 was 0.6 ± 0.2 s^{-1}.

Possible Causes of Carrier Transport in the Au−S−$(CH_2)_2$-ds-oligo-NH−PQQCH_2, but Not in the Au−S−$(CH_2)_2$-ss-oligo-NH−PQQ layer, nor in the SBP-Doped Disordered ds-Calf Thymus DNA Film. Possible hypotheses explaining the apparent carrier transport in the ds-oligonucleotide monolayer include, but are not limited to, the following:

(a) Each helix conducts electrons, acting as a "wire"; conductivity is an intrinsic property of the ds-DNA molecule.

(b) Conductivity in thin solid films of ds-DNA is a colligative property of an ensemble of aligned helices. The alignment of helices in ds-DNA aggregate results in the formation of a one-dimensional semiconductor, just as the ordering of silicon atoms in connected tetrahedra results in the formation of semiconducting silicon. The Bohr radius of a "dopant" of the semiconducting ds-DNA film is large because the high-frequency longitudinal dielectric constant of ds-DNA is large. The large high-frequency longitudinal dielectric constant results of the large high-frequency longitudinal polarizability of ds-DNA,[70] itself the result of the concerted shift of cations between nearby phosphate functions of the helix, along the long axes of the aligned helices, in an electric field. The donors in the ds-DNA films are reversibly electrooxidized functions of ds-DNA. The ionization energy of donors approaches kT when the longitudinal high-frequency dielectric constant is high.

(c) Neither the ds-DNA helices nor their aggregates conduct electrons or holes. Conduction results instead of electron-exchanging collisions between flexible spacer arm-tethered, but mobile, terminal PQQ functions. The collisions enable lateral transport of electrons or holes in thin films of ds-DNA. The electrons or holes drop to the gold surface upon reaching a defect in the monolayer, such as a pinhole.

If hypothesis *a* were valid, the expected enhanced, electrical communication between soybean peroxidase and the gold surface should have resulted in enhanced electrocatalytic reduction of H_2O_2. Such enhancement was, however, not observed.

According to hypothesis *b*, the underlying cause of carrier transport is the high-frequency longitudinal dielectric constant (in reality dielectric function) ϵ_∞, which is high when the ds-DNA rods are aligned. That the alignment of the helices results in anisotropic polarizability, and that the polarizability leads to electric dichroism and to birefringence in DNA solutions[9−24] and to ferroelectric behavior in solid DNA films[25] is well recognized. Hypothesis *b* is also consistent with results showing that upon chain alignment the conductivity of ds-DNA films increases drastically in the direction of the long axes of the helices,[7] with the semiconductor-like behavior of "ropes" of DNA,[6] and possibly also with the requirement of the presence of G-bases in dissolved molecular electron-transferring ds-DNA.[33,34] In the framework of hypothesis *b*, G of the GC base pair is ionized in a medium with a large high-frequency dielectric constant[70] and behaves as an ionized donor in the one-dimensionally semiconducting ds-DNA.

Lateral electron transfer in monolayers, which underlies hypothesis *c*, is well-established.[71−73] Lateral electron transport and drainage through pinholes are, however, inconsistent with

(70) Kittel, C. *Introduction to Solid State Physics*, 5th ed.; Wiley: New York, 1976; p 232.

(71) Widrig, C. A.; Miller, C. J.; Majda, M. *J. Am. Chem. Soc.* **1988**, *110*, 2009.

(72) Charych, D. H.; Majda, M. *Thin Solid Films* **1992**, *210−211*, 348.

(73) Charych, D. H.; Anvar, D. J.; Majda, M. *Thin Solid Films* **1994**, *242*, 1.

• the observed reduction in the rate of carrier transport upon introduction of mismatched base pairs,

• the helix footprint-defined large (35 Å) average distance between the ds-oligonucleotide bound PQQ redox functions,

• the persistence of the faradaic process upon reducing the redox species concentration in the oligonucleotide contacting layer from ≥0.15 M (one PQQ function tethered to each helix) to ≤10 mM [$(Fe(CN)_6)^{3-/4-}$ electrostatically repelled from the oligonucleotide contacting layer], and

• the conventional, rather than microarray electrode characteristics[61] of the voltammograms.

Lateral electron transport has been reported thus far only in monolayers that were at least 10-fold more densely packed with fast redox functions than the ds-oligonucleotide monolayers. In the ds-oligonucleotide monolayers the distance between the redox functions was defined by the 35 Å diameters of the double helices, each of which had a single terminal redox function. Their separation may be contrasted with the about 15 Å maximal electron-transfer distance in proteins and across insulating monolayers. Because in proteins and in insulating thiol-terminated hydrocarbon monolayers on gold the rate of electron-transfer drops by about a factor of *e* per each 1 Å increase in separation, the rate for each electron-transferring step would have been a factor of $>10^6$ smaller than that in an electron-transferring protein. Furthermore, not one, but several of these steps would have been required for the electron to be drained in a pinhole.

Nonetheless, because the PQQ redox functions were tethered to the oligonucleotide by an eight-atom long spacer arm, comprising both flexible and rigid domains, transport of electrons through a quasi-diffusional process merits consideration. In such a process neighboring redox functions at the termini of flexible tethers periodically approach each other and exchange electrons. The process requires that the self-exchange for PQQ be fast. Its rate is expected to scale with the frequency of collisions and therefore with the square of the concentration of the colliding and thereby self-exchanging redox species. The concentration of PQQ in the maximally ∼1 nm thick slab containing the PQQ (terminally tethered to the ds-oligonucleotide of the monolayer) was ∼0.15 M. (If a thinner slab were assumed, the concentration would have been higher.) The Faradaic process persisted, however, when the tethered PQQ was replaced by 10 mM $Fe(CN)_6^{3-/4-}$, an anion excluded from the immediate proximity of the polyanionic monolayer. The fact that the Faradaic process persisted in 10 mM $Fe(CN)_6^{3-/4-}$, and that the PQQ−ds-oligonucleotide monolayer and the ds-oligonucleotide monolayer/10 mM $Fe(CN)_6^{3-/4-}$/voltammograms were similar at equal scan rate establishes that the Faradaic reaction was not particularly sensitive to the concentration of the redox species. Recall here that the nonhybridized ss-oligonucleotide monolayers perfectly blocked the electrooxidation and the electroreduction of both freely diffusing $Fe(CN)_6^{3-/4-}$ and of tethered PQQ. We thus consider the persistence of the Faradaic reaction and of its voltammetric characteristics upon replacing the tethered PQQ with 10 mM $Fe(CN)_6^{3-/4-}$ to be inconsistent with lateral transport and drainage of electrons through pinholes.

The absence of microarray electrode characteristics from the voltammograms adds further evidence against a pinhole-dependent electrode reaction. Finklea, Rubinstein, and their co-workers have shown that pinholes in an octadecanethiol monolayer on gold produce unique voltammetric characteristics, resembling those of dot microarrays.[61] The observed voltammograms of the ds-oligonucleotide monolayers, whether with diffusing $Fe(CN)_6^{3-/4-}$ or with tethered PQQ, were, however, conventional.

Thus, of the three hypotheses, only hypothesis *b* is consistent with all of the results of this study and those of two earlier ones.[6,7]

Effect of the Magnitude of ϵ_∞. We start by considering the effect of the dielectric constant on the Bohr radius and on the ionization energy of a dopant in an isotropic nonpolar, cubic semiconductor; we then review Mott and Gurney's treatment of electronic conduction in ionic crystals showing that the critical parameter defining carrier transport is the difference between the static and high-frequency dielectric constants. When this difference diminishes and if the absolute magnitude of the high frequency dielectric constant associated with longitudinal, not the transverse, polarization is still reasonably high (>10), then the carriers are mobile in polar lattices. We then consider the polarizability of an array of aligned DNA molecules, pointing out that in KDP (potassium dihydrogen phosphate) concerted movement of cations results in a high longitudinal polarizability, in a high-frequency dielectric constant, and is the cause of these crystals being ferroelectric. We cite earlier work showing that double-stranded DNA is similarly polarizable when its helices are aligned, the polarization resulting in dielectric birefringence in solution and in ferroelectric domains in films. We then point out that the high longitudinal polarizability, resulting from concerted movement of cations, raises the high-frequency dielectric constant in the direction of the long axes of the helices. This, combined with only part of the volume in the hydrated film being occupied by water, reduces the difference between the static and high-frequency longitudinal dielectric constants and enables the transport of carriers. Finally, we propose that the relatively easy to oxidize G-residues of GC base pairs in ds-DNA behave as donors and are ionized when the high-frequency dielectric constant is high. Their ionization makes the aligned chains one-dimensional conductors, the conduction being confined to the direction of the long axes of the helices and being a colligative property of the aligned polarizable array.

In a doped nonpolar semiconductor, like silicon or germanium, conductivity derives of the small ionization energy and large Bohr radius of a dopant. The radii r_0 (eq 5) scale with the dielectric constant[70] according to

$$r_0 = \epsilon\hbar^2/(e^2 m_e) \tag{5}$$

where ϵ is the dielectric constant (the ratio of the permittivity to that in vacuo) $\hbar$ is Heisenberg's constant, *e* is the charge of the electron, and m_e is the effective electron mass. The radii are typically of 30−100 Å when the dielectric constants are between 10 and 20.

The ionization energies of the donors scale with the inverse of the square of the dielectric constant[70] according to eq 6

$$E_g - E_d = e^4 m_e/(2\epsilon^2\hbar^2) \tag{6}$$

Their typical values are of tens of meVs, on the order of *kT* at ambient temperatures. Because their donors are ionized, highly donor-doped semiconductors are good electron conductors at room temperature.

DNA Films Are Ionic Solids. The classical treatise on electronic properties of ionic solids is that of N. F. Mott and R. W. Gurney.[74] Their book contains two chapters that are particularly relevant to the electronic properties of DNA: chapter I considers the longitudinal polarizability, the high-frequency dielectric constant of an ionic lattice, and its static

(74) Mott, N. F.; Gurney, R. W. *Electronic Processes in Ionic Crystals*, 2nd ed.; Oxford University Press: New York, 1950; pp 25, 82, 107.

dielectric constant; chapter III considers electrons in a polar crystal including the mean free path of an electron and its mobility in an ionic solid. It shows that ionic crystals become conductive if doped and if the mean free path of the electrons exceeds the dimensions of the lattice constant a_0. According to Mott and Gurney, the mean free path and the mobility of the electrons scale with

$$a_0\,(\epsilon_\infty - \epsilon_0 + 1)/(\epsilon_\infty - \epsilon_0) \qquad (7)$$

where ϵ_0 is the static dielectric constant. Usually, in ionic solids, the difference is large. However, in aligned ds-DNA films the difference is reduced because the large longitudinal high frequency polarizability. The large polarizability results of the concerted shift in the positions of the DNA's phosphate-charge-balancing cations in an electric field. It increases only the resolved component of ϵ_∞ in the direction of the long axes of the helices. The literature is rich in data of the dielectric constant (function), relaxation, and loss of ds-DNA solutions, but data for thin solid films made of aligned ds-DNA helices are scarce. On the basis of measurements of Takashima,[75] Hornick and Weill[10] estimated that the longitudinal low-frequency dielectric constant of ds-DNA was large, as high as 190 000. Takashima provided transverse, but not longitudinal, values of ϵ_∞ and of ϵ_0 for thymus ds-DNA solutions in shear gradients causing chain alignment.[11] Goswami and Gupta[76] reported a value of $\epsilon_\infty = 82$ at 100 kHz for ds-DNA and also reported a particularly short dielectric relaxation time of 0.2 ms. We note that the anisotropic ϵ_∞ is 46 for the *c*-axis of potassium dihydrogen phosphate (KDP), one of the best studied ferroelectrics. KDP is polarized, like ds-DNA, by the concerted shift of the phosphate charge balancing cations by one lattice constant. ϵ_∞ is also high in other ferroelectric, hydrogen-containing phosphates and arsenates. In these, as in the ds-DNA, polarization results of protonating or adding a sodium cation to one side of a lattice and deprotonating or dissociating the sodium cation at the opposite side. The apparently high anisotropic polarizability of ds-DNA explains why Vasilescu[25] found ferroelectric behavior in aligned DNA films and why Laudat et al. reported polarization-caused electret-like behavior in ds-DNA.[77]

We note that the proposed conduction differs from that of polarons in two ways; first, the Bohr orbitals of ionized donors in ds-DNA are sausage-like and tens of Å long. The electrons are effectively delocalized, neither trapped by polarizing their environment, nor hopping from trap-to-trap. Second, the longitudinal polarization of the ds-DNA rods does not involve a change in the coordinates of any atom in the array, involving merely the adding of a proton or sodium ion to one side and its removal at the other, a process that may be described as changing coordinates of atoms in two terminal water molecules in the case of protons and as terminal ion pairing and dissociation in the case of sodium cations. In this context Fornés[78] estimates for ds-DNA a terminally fluctuating dipole moment which is 4×10^5 times greater than the permanent dipole moment of water at room temperature, and Ookubo et al.[79] point out that the longitudinal dielectric relaxation of ds-DNA is much faster than of other polyelectrolytes.

We emphasize that our considerations apply to solid DNA films, not to discrete DNA molecules in solution; that ϵ_∞ of the films cannot be high unless the helices are aligned and that when the ds-helices are aligned, only the resolved component of the high-frequency dielectric constant in the direction of the long axes is high, wherefore the mean free path and mobility of electrons is high only along the helices; that, even if aligned, only films doped with a donor or with an acceptor can conduct; and that the doped ds-DNA films can conduct only in one direction, along the long axes of the helices.

We note that though donor ionization energies and electrooxidation potentials are related, their reactions and their values differ; ionization, unlike electrooxidation, does not involve displacement of ions. We do not know of electrochemical data that would suggest a reversibly reducible, and thus electron-capturing function in DNA that could be an acceptor, or a p-type dopant. We have, therefore, no basis to suggest the possibility of p-type conduction. We do know, however, of one function that may be reversibly ionized in a medium with a high-dielectric constant ϵ_∞ and may act as n-type dopant. This is the G-residue of DNA in the GC base pair of the helix.[80−82] The G base is the easiest to electrooxidize,[80,81] and the forming of the GC base pair further facilitates its oxidation/ionization.[82] Consequently, it is possible that the observed decrease in k_0 upon the introduction of the two mismatches through CC → AT substitution was caused by the increased threshold for oxidation/ionization of the GG residues of the complementary strand, which were paired in the perfect hybrid but not in the hybrid with the two mismatched base pairs.

We do not know at this time whether uniaxial electron conduction in films consisting of aligned ds-DNA molecules, a colligative property, and long-range electron transfer in solutions of ds-DNA, apparently a molecular property, are related. We note, however, that the presence of G-residues is a condition for long-range electron transfer in dissolved ds-DNA.[35,36]

Biological significance of electron conduction in aligned ds-DNA aggregates. Alignment, leading to electron conduction, stabilizes ds-DNA aggregates against damage by oxidation or reduction. Removal of electrons from or addition of electrons to a non-conducting polymer oxidize or reduce the polymer when followed by a step involving the transport of ions, thus resulting in its chemical reaction. For example, one-electron oxidation or reduction of a polymer that does not conduct electrons or holes, creates a reactive radical. In ds-DNA such oxidation or reduction leads to the well-researched impairment of the information stored. In contrast, the addition or removal of an electron or of a hole does not lead to a chemical change in a donor or acceptor-doped semiconductor, and addition or removal of one electron does not produce a reactive radical. Because the band from which the charge carrier is removed, or the one to which it is added, extends in a semiconductor over the entire lattice, no individual atom or function becomes uniquely reactive. Thus, parallel alignment of the ds-DNA segments in a long double helix or lining up in parallel multiple ds-DNA molecules, either of which will make a one (or higher)-dimensional semiconductor, is likely to reduce the likelihood of damage by oxidation (and also by reduction). Organisms

(75) Takashima, S. *Adv. Chem. Ser.* **1967**, *63*, 232.
(76) Goswami, D. N.; Das Gupta, N. N. *Biopolymers* **1974**, *13*, 1549.
(77) Laudat, J.; Jelinkova, E.; Neubert, M.; Bakule, R.; Nedbal, J.; Prosser, V. *Mater. Sci.* **1984**, *10*, 177.
(78) Fornés, J. A. *Phys. Rev. E* **1998**, *57*, 2110.
(79) Ookubo, N.; Hirai, Y.; Ito, K.; Hayakawa, R. *Macromolecules* **1989**, *22*, 1359.
(80) Brett, C. M. A.; Brett, A. M. O.; Serrano, S. H. P. *J. Electroanal. Chem.* **1994**, *366*, 225.
(81) Tomschik, M.; Jelen, F.; Harran, L.; Trnkova, L.; Nielsen, P. E.; Palacek, E. *J. Electroanal. Chem.* **1999**, *476*, 71.
(82) Hutter, M.; Clark. T. *J. Am. Chem. Soc.* **1996**, *118*, 7574.
(83) Wolf, S. G.; Frenkel, D.; Arad, T.; Finkel, S. E.; Kolter, R.; Minsky, A. *Nature*, **1999**, *400*, 83.
(84) The geometry was optimized with "PCSPARTAN".
(85) Guckian, K. M.; Schweitzer, B. A.; Ren, R. X.-F.; Sheils, C. J.; Paris, P. L.; Tahmassebi, D. C.; Kool, E. T. *J. Am. Chem. Soc.* **1996**, *118*, 8182.

might use alignment to protect their DNA when passing from an active-growth or multiplicative phase to a protective or inactive-dormant stage, for example upon change in the environment's temperature or chemical composition. Indeed, Wolf et al.[83] recently reported a generic process of stress-induced crystallization of ds-DNA in *E. coli*. When stressed, the organism protects its DNA by generating a protein *Dsp* that rapidly co-crystallizes with ds-DNA. In the *Dsp*-ds-DNA lattice the *Dsp* occupy alternating layers, the lattice having pure ds-DNA sheets, in which the DNA molecules are aligned. According to the model of this paper, such a lattice would conduct electrons in the direction of the long axes of the aligned helices. We consider it likely that the organization of ds-DNA in aligned, polarizable arrays will prove to be a central evolutionary strategy for preserving genetic information. Alignment is particularly expected in the life cycle of cells and organisms when their DNA is particularly exposed and when it becomes vulnerable in a changed environment.

Conclusions

The results on the calf thymus DNA-containing films suggest that randomly oriented ds-DNA does not conduct electrons or holes. The results of Fink and Schönenberger,[6] of Okahata,[7] and of this study appear to be consistent with a doped ionic semiconductor model. According to this model, the cause of donor ionization and carrier mobility is the reduced difference between the static and high frequency longitudinal dielectric constants, resolved in the direction of the long axes of the helices, in aligned ds-DNA films. Whether or not this model is valid will only be known after the values of the two constants are measured. The model leads, however, to some verifiable predictions: first, if the ds-DNA helices are aligned by polarizing their films on densely spaced interdigitated comb electrodes, one expects to observe steady-state electron transport after the ionic current decays. Second, because polarization involves the concerted movement of cations, deuterium exchange is expected to affect the conductivity. Deuterium exchange increases the dielectric constant (from 46 to 88) and raises the curie temperature (from 123 K to 213 K) in ferroelectric potassium dihydrogen phosphate; third, upon alignment of the ds-DNA in a direction perpendicular to the surface of the electrode, peroxidases bound to the solution-side DNA termini are expected to be "wired". The oxidized peroxidase molecules would act as p-type dopants and which make the films conductive even if they consisted only of A and T, but contained no G (donor) residues.

Acknowledgment. This work was supported by the Deutsche Forschungsgemeinschaft (Aktenzeichen HA 2231/3-1 -3/2), the National Science Foundation, and the Robert A. Welch Foundation. The authors acknowledge with gratitude discussions with Professor Israel Rubinstein. Professor Abraham Minsky brought to their attention his observation of stress induced biocrystallization of ds-DNA in *E. coli*.

JA9920664